

Joint Waveform and Beamforming Optimization for MIMO Wireless Power Transfer

Shanpu Shen, *Member, IEEE*, and Bruno Clerckx, *Senior Member, IEEE*

Abstract—In this paper, we study a multi-sine multiple-input multiple-output (MIMO) wireless power transfer (WPT) system with the objective to increase the output DC power. We jointly optimize the multi-sine waveform and beamforming accounting for the rectenna nonlinearity, and consider two combining schemes for the rectennas at the receiver, namely DC and RF combinings. For DC combining, the waveform and transmit beamforming are optimized, as a function of the channel state information (CSI). For RF combining, the optimal transmit and receive beamformings are provided in closed form and the waveform is optimized. We also consider a practical RF combining circuit using phase shifter and RF power combiner and optimize the waveform, transmit beamforming, and analog receive beamforming adaptive to the CSI. Two types of performance evaluations, based on the nonlinear rectenna model and accurate and realistic circuit simulations, are provided. The evaluations demonstrate that the joint waveform and beamforming design can increase the output DC power by leveraging the beamforming gain, the frequency diversity gain, and the rectenna nonlinearity. It also shows that the joint waveform and beamforming design provides a higher output DC power than the beamforming-only design with a relative gain of 180% in a two-transmit antenna sixteen-sine wave two-receive antenna setup.

Index Terms—Beamforming, DC combining, MIMO, multi-sine, nonlinearity, optimization, RF combining, waveform, wireless power transfer.

I. INTRODUCTION

WIRELESS power transfer (WPT) has a long history and nowadays attracts more and more attentions as a promising energy harvesting technology. Near-field WPT via inductive coupling has been utilized for charging cell phones, medical implants, and electrical vehicles, but the limitation is that it can only transfer power in a very short distance. In contrast with the near-field WPT, far-field WPT via radio frequency (RF) enables a long-distance power transfer to energize numerous devices in the Internet of Things (IoT) [1]. The far-field WPT utilizes a dedicated source to radiate RF energy through a wireless channel and a rectifying antenna (rectenna) at the receiver to receive and convert this energy into DC power. In contrast to batteries that need to be replaced and recharged periodically, far-field WPT provides a more reliable, controllable, user-friendly, and cost-effective way to power the devices in the IoT. Furthermore, the far-field WPT can be extended to simultaneous wireless information and power transfer (SWIPT) resulting in significant gains in terms

of spectral efficiency and energy efficiency by superposing information and power transfer [2]. The major challenge of far-field WPT is to increase the output DC power of rectenna without increasing the transmit power. To solve this challenge, a large amount of the technical efforts in the literature have been devoted to designing efficient rectennas [3], [4].

Designing efficient WPT signals and waveforms can also increase the output DC power [1]. Multi-sine signal excitation [5] has been shown through RF measurements to increase the RF-to-DC conversion efficiency and therefore increase the output DC power. However, the main limitation of the method is not only the lack of a systematic approach to design waveforms, but also the fact that they operate without Channel State Information (CSI) at the Transmitter (CSIT) and Receiver (CSIR). The first systematic analysis, design and optimization of waveforms for WPT was conducted in [6]. Those waveforms are adaptive to the CSI and jointly leverage the beamforming gain, the frequency selectivity of the channel, and the rectenna nonlinearity to maximize the output DC power. Since then, further enhancements have been made to waveform optimization adaptive to CSI with the objective to reduce the design complexity and extend to large scale multi-antenna multi-sine WPT [7]-[10], to account for limited feedback [11], to energize multiple devices (multi-user setting) [7], [12], to transfer information and power simultaneously [13]-[15], and to enable efficient wireless powered communications [16], [17].

In addition to designing efficient rectenna and waveform, using multiple rectennas, also known as multiport rectennas, at the receiver to form a multiple-input multiple-output (MIMO) WPT system can effectively increase the output DC power. This contrasts with all prior works [6]-[17] that assumed a single rectenna per device. Interestingly, multiport rectennas have been designed in [18]-[23] for ambient RF energy harvesting, which is similar to WPT but does not have a controllable and dedicated transmitter. It was shown that using multiport rectennas can linearly increase the output DC power with the number of rectennas at the receiver. DC combining and RF combining for the multiple rectennas at the receiver have been investigated in [24], but the investigation is at the level of RF circuit design and does not consider the impact on communication and signal designs including adaptive waveform and beamforming optimization.

Systematic studies of MIMO WPT systems were conducted in [25]-[27]. In [25], a general design framework for channel acquisition was proposed for MIMO WPT systems with limited feedback, but the limitation is that it does not consider 1) the rectenna nonlinearity, 2) RF combining, and 3) waveform

Manuscript received; This work was supported in part by the EPSRC of U.K. under Grant EP/P003885/1 and EP/R511547/1. (*Corresponding author: Shanpu Shen.*)

The authors are with the Department of Electrical and Electronic Engineering, Imperial College London, London SW7 2AZ, U.K. (e-mail: s.shen@imperial.ac.uk; b.clerckx@imperial.ac.uk).

design, which are all beneficial to increase the output DC power. In [26], a generic receiver architecture for MIMO WPT systems was proposed. The generic receiver architecture leverages the rectenna nonlinearity by using a sigmoidal function-based rectenna model to maximize the output DC power, but the limitation is that it only focuses beamforming design and does not consider the waveform design. More recently, in [27], a systematic beamforming design and optimization for MIMO WPT with DC and RF combining was proposed. As a result of the rectenna nonlinearity (modeled based on a Taylor expansion of the diode I-V characteristics), [27] has shown that RF combining provides significant performance benefits over DC combining, though results in a more complex architecture where transmit and receive beamformings have to be jointly optimized. Though [27] sheds some new light on beamforming design for MIMO WPT with various combining, its design is limited by the use of continuous sinewave. In view of the recent results in [27] and past results on waveform design for WPT [6], [7], we go one step further and ask ourselves how to design an even more efficient WPT architecture by jointly optimizing the waveform and beamforming in a MIMO WPT.

In this paper, we consider the joint design of waveform and beamforming for MIMO WPT systems, accounting for the rectenna nonlinearity to increase the output DC power. This is the first paper to jointly optimize the waveform and beamforming for MIMO WPT systems. The contributions of the paper are summarized as follow.

First, we analyze a multi-sine MIMO WPT architecture with joint waveform and beamforming optimization, accounting for the rectenna nonlinearity. Two combining schemes, DC and RF combinings, for the multiple rectennas at the receiver are considered.

Second, for DC combining, assuming perfect CSIT and leveraging the nonlinear rectenna model, we jointly optimize the waveform and transmit beamforming in the multi-sine MIMO WPT system with the objective to maximize the total output DC power of all rectennas. The waveform and beamforming are optimized with guarantee of converging to a stationary point by using successive convex approximation (SCA) and semidefinite relaxation (SDR).

Third, for RF combining, assuming perfect CSIT and CSIR and leveraging the nonlinear rectenna model, we optimize the waveform and transmit and receive beamformings in the multi-sine MIMO WPT system with the objective to maximize the output DC power. The optimal transmit and receive beamformings are provided in closed form, while the waveform optimization is formulated as a nonconvex posynomial maximization problem and solved with guarantee of converging to a stationary point by using SCA.

Fourth, a practical RF combining circuit consisting of phase shifters and an RF power combiner is considered for the multi-sine MIMO WPT system. Assuming perfect CSIT and CSIR and leveraging the nonlinear rectenna model, the waveform, transmit beamforming, and analog receive beamforming are jointly optimized with the objective to maximize the output DC power. The optimization is solved with guarantee of converging to a stationary point by using SCA.

Fifth, the joint waveform and beamforming optimization

for DC and RF combinings are shown to increase the output DC power through an accurate and realistic circuit evaluation. Comparison with the waveform and beamforming design optimized with the linear rectenna model is also provided to show the crucial role played by the rectenna nonlinearity in WPT. In addition, compared with the beamforming only design proposed by [27], the proposed joint waveform and beamforming design is shown to have a relative gain in terms of the output DC power which can exceed 100% when there are sixteen sinewaves and can reach to 180% in a two-transmit antenna sixteen-sinewave two-receive antenna setup. Moreover, it is shown that RF combining provides a higher output DC power than DC combining since it can leverage the rectenna nonlinearity more efficiently.

In contrast with [27] which assumes a continuous sinewave and only considers beamforming design, this paper tackles the joint waveform and beamforming design. Such a joint waveform and beamforming design leads to a significantly enhanced performance. However, it is important to note that the joint waveform and beamforming design also brings new challenges including: 1) The MIMO WPT system model is more complex when the multi-sine waveform is considered. 2) The optimization objective function, i.e. the output DC power, has a much more complex expression. Due to the rectenna nonlinearity, the received RF signals at different frequencies are coupled with each other in the expression of the output DC power, which makes the optimization a NP-hard problem. 3) The optimization involves more variables across frequency (for waveform) and space (for beamforming). These variables cannot be uncoupled in the optimization and have to be jointly optimized, which increase the optimization complexity. Furthermore, it is also important to highlight that the algorithms for beamforming only design in [27] cannot guarantee finding a stationary point due to using SDR (only numerically guarantee for tested channels), however, the algorithms proposed in this paper not only generalize the beamforming only design but also has an advancement that it can theoretically guarantee finding a stationary point.

Organization: Section II introduces the multi-sine MIMO WPT system model and Section III briefly revisits the nonlinear rectenna model. Section IV and Section V tackle the joint waveform and beamforming optimization for DC and RF combinings, respectively. Section VI evaluates the performance and Section VII concludes the work.

Notations: Bold lower and upper case letters stand for vectors and matrices, respectively. A symbol not in bold font represents a scalar. $\mathcal{E}\{\cdot\}$ refers to the expectation/averaging operator. $\Re\{x\}$ and $|x|$ refer to the real part and modulus of a complex number x , respectively. $\|\mathbf{x}\|$ and $[\mathbf{x}]_i$ refer to the l_2 -norm and i th element of a vector \mathbf{x} , respectively. $\arg(\mathbf{x})$ refers to a vector with each element being the phase of the corresponding element in a vector \mathbf{x} . \mathbf{X}^T , \mathbf{X}^H , $\text{Tr}(\mathbf{X})$, and $\text{rank}(\mathbf{X})$ refer to the transpose, conjugate transpose, trace, and rank of a matrix \mathbf{X} , respectively. $\mathbf{X} \succeq \mathbf{0}$ means that \mathbf{X} is positive semidefinite. $\mathbf{0}$ denotes an all-zero vector. \log is in base e .

II. MULTI-SINE MIMO WPT MODEL

We consider a point-to-point multi-sine MIMO WPT system. There are M antennas at the transmitter and Q antennas at the receiver. A multi-sine waveform over N angular frequencies $\omega_1, \omega_2, \dots, \omega_N$ is transmitted. The multi-sine waveform transmitted by the m th transmit antenna is given by

$$x_m(t) = \Re \left\{ \sum_{n=1}^N s_{m,n} e^{j\omega_n t} \right\} \quad (1)$$

where $s_{m,n}$ is a complex weight accounting for the magnitude and phase of the n th sinewave on the m th transmit antenna. We group $s_{m,n}$ into a M -dimensional vector $\mathbf{s}_n = [s_{1,n}, s_{2,n}, \dots, s_{M,n}]^T$. We further group $\mathbf{s}_n \forall n$ into a MN -dimensional vector $\mathbf{s} = [\mathbf{s}_1^T, \mathbf{s}_2^T, \dots, \mathbf{s}_N^T]^T$. The transmitter is subject to a transmit power constraint given by

$$\frac{1}{2} \|\mathbf{s}\|^2 \leq P \quad (2)$$

where P denotes the transmit power. We group $x_m(t)$ into $\mathbf{x}(t) = [x_1(t), x_2(t), \dots, x_M(t)]^T$ and it can be rewritten as

$$\mathbf{x}(t) = \Re \left\{ \sum_{n=1}^N \mathbf{s}_n e^{j\omega_n t} \right\}. \quad (3)$$

The multi-sine waveform transmitted by the multiple transmit antennas propagate through a wireless channel. The received signal at the q th receive antenna can be expressed as

$$y_q(t) = \Re \left\{ \sum_{n=1}^N \mathbf{h}_{q,n} \mathbf{s}_n e^{j\omega_n t} \right\} \quad (4)$$

where $\mathbf{h}_{q,n} = [h_{q,1,n}, h_{q,2,n}, \dots, h_{q,M,n}]$ with $h_{q,m,n}$ referring to the complex channel gain between the m th transmit antenna and the q th receive antenna at the n th angular frequency. We collect all $\mathbf{h}_{q,n}$ into a matrix $\mathbf{H}_n = [\mathbf{h}_{1,n}^T, \mathbf{h}_{2,n}^T, \dots, \mathbf{h}_{Q,n}^T]^T$ where \mathbf{H}_n represents the $Q \times M$ channel matrix at the n th angular frequency of the multi-sine MIMO WPT system. We assume that the channel matrix \mathbf{H}_n is perfectly known to the transmitter and the receiver.

In this paper, we optimize \mathbf{s} with the transmit power constraint (2) to maximize the output DC power of multi-sine MIMO WPT systems. At the n th sinewave, \mathbf{s}_n characterizes the beamforming for the multiple transmit antennas, so that optimizing \mathbf{s} includes the beamforming optimization. On the other hand, at the m th transmit antenna, $s_{m,1}, s_{m,2}, \dots, s_{m,N}$ characterize the multi-sine waveform $x_m(t)$, so that optimizing \mathbf{s} includes the waveform optimization. It should be noted that the waveform optimized in this paper is multi-sine waveform at fixed N angular frequencies, not waveform with arbitrary spectrum. Therefore, optimizing \mathbf{s} means the joint waveform and beamforming optimization.

III. RECTENNA MODEL

We briefly revisit a rectenna model derived in the past literature [7]. The model accounts for the rectenna nonlinearity through the higher order terms in the Taylor expansion of the

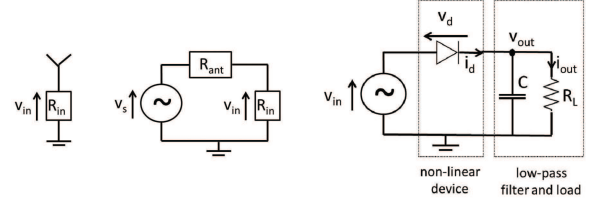


Fig. 1. Antenna equivalent circuit (left) and a single diode rectifier (right).

diode I-V characteristics while having a simple and tractable expression¹.

Consider a rectifier with input impedance R_{in} connected to a receive antenna as shown in Fig. 1. The signal $y(t)$ impinging on the antenna has an average power $P_{av} = \mathcal{E} \{ y(t)^2 \}$. The receive antenna is assumed lossless and modeled as an equivalent voltage source $v_s(t)$ in series with an impedance $R_{ant} = 50 \Omega$ as shown in Fig. 1. With perfect matching ($R_{in} = R_{ant}$), the input voltage of the rectifier $v_{in}(t)$ can be related to the received signal $y(t)$ by $v_{in}(t) = y(t) \sqrt{R_{ant}}$. A rectifier is always made of a nonlinear rectifying component such as a diode followed by a low pass filter with a load [19], [21], [22], as shown in Fig. 1. The current $i_d(t)$ flowing through an ideal diode (neglecting its series resistance) relates to the voltage drop across the diode $v_d(t) = v_{in}(t) - v_{out}(t)$ as $i_d(t) = i_s \left(e^{\frac{v_d(t)}{n_i v_t}} - 1 \right)$ where i_s is the reverse bias saturation current, v_t is the thermal voltage, n_i is the ideality factor (assumed equal to 1.05).

In [7], by assuming zero output DC current and taking Taylor expansion at zero quiescent point to the n_0 th-order term, the output DC voltage of the rectifier v_{out} is approximated as

$$v_{out} = \sum_{i \text{ even}, i \geq 2}^{n_0} \beta_i \mathcal{E} \{ y(t)^i \} \quad (5)$$

where $\beta_i = \frac{R_{ant}^{i/2}}{i!(n_i v_t)^{i-1}}$. There is no odd (first, third, and fifth, etc) order terms in the output DC voltage (5) because $\mathcal{E} \{ y(t)^i \} = 0$ for i odd, i.e. odd order terms have zero mean, which has also been shown in [6]. In the following Sections, we mainly consider the truncation order $n_0 = 4$ since $n_0 = 4$ is a good choice [7].

IV. JOINT WAVEFORM AND BEAMFORMING OPTIMIZATION WITH DC COMBINING

Consider the DC combining scheme for the multiple receive antenna system as shown in Fig. 2. Each receive antenna is connected to a rectifier so that the RF signal received by each antenna is individually rectified. Using the nonlinear rectenna model (5) with the truncation order $n_0 = 4$, the output DC voltage of the q th rectifier (connected to the q th receive antenna) is given by

$$v_{out,q} = \beta_2 \mathcal{E} \{ y_q(t)^2 \} + \beta_4 \mathcal{E} \{ y_q(t)^4 \}, \quad (6)$$

¹There is another nonlinear rectenna model proposed in [28], however, the model in [28] cannot be used for waveform optimization. A detailed comparison between the model in [7] and the model in [28] is provided in [13], [29].

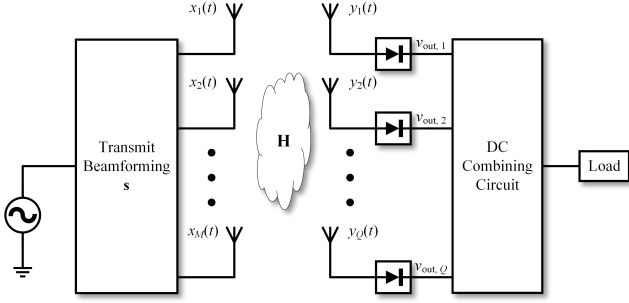


Fig. 2. Schematic of the multi-sine MIMO WPT system with DC combining in the receiver.

$$\mathbf{M}_q = \begin{pmatrix} \mathbf{h}_{q,1}^H \mathbf{h}_{q,1} & \mathbf{h}_{q,1}^H \mathbf{h}_{q,2} & \mathbf{h}_{q,1}^H \mathbf{h}_{q,3} & \dots & \mathbf{h}_{q,1}^H \mathbf{h}_{q,N} \\ \mathbf{h}_{q,2}^H \mathbf{h}_{q,1} & \mathbf{h}_{q,2}^H \mathbf{h}_{q,2} & \mathbf{h}_{q,2}^H \mathbf{h}_{q,3} & \dots & \mathbf{h}_{q,2}^H \mathbf{h}_{q,N} \\ \mathbf{h}_{q,3}^H \mathbf{h}_{q,1} & \mathbf{h}_{q,3}^H \mathbf{h}_{q,2} & \mathbf{h}_{q,3}^H \mathbf{h}_{q,3} & \dots & \mathbf{h}_{q,3}^H \mathbf{h}_{q,N} \\ \vdots & \vdots & \vdots & \ddots & \vdots \\ \mathbf{h}_{q,N}^H \mathbf{h}_{q,1} & \dots & \dots & \dots & \mathbf{h}_{q,N}^H \mathbf{h}_{q,N} \end{pmatrix} \begin{matrix} \leftarrow k = -1 \\ \\ \\ \\ \leftarrow k = 1 \\ \leftarrow k = 0 \end{matrix}$$

Fig. 3. $\mathbf{M}_{q,1}$ is the above matrix only maintaining the block diagonal (whose index is $k = 1$) in pink, while all the other blocks are set as zero matrices.

where $\mathcal{E}\{y_q(t)^2\}$ and $\mathcal{E}\{y_q(t)^4\}$ are given by

$$\mathcal{E}\{y_q(t)^2\} = \frac{1}{2} \sum_{n=1}^N \mathbf{s}_n^H \mathbf{h}_{q,n} \mathbf{h}_{q,n}^H \mathbf{s}_n, \quad (7)$$

$$\mathcal{E}\{y_q(t)^4\} = \frac{3}{8} \sum_{\substack{n_1, n_2, n_3, n_4 \\ n_1 + n_2 = n_3 + n_4}} (\mathbf{s}_{n_3}^H \mathbf{h}_{q,n_3} \mathbf{h}_{q,n_1} \mathbf{s}_{n_1} \cdot \mathbf{s}_{n_4}^H \mathbf{h}_{q,n_4} \mathbf{h}_{q,n_2} \mathbf{s}_{n_2}). \quad (8)$$

We can rewrite $v_{out,q}$ in a more compact form by introducing MN -by- MN matrices \mathbf{M}_q and $\mathbf{M}_{q,k}$. \mathbf{M}_q is defined by $\mathbf{M}_q \triangleq \mathbf{h}_q^H \mathbf{h}_q$ with $\mathbf{h}_q = [\mathbf{h}_{q,1}, \mathbf{h}_{q,2}, \dots, \mathbf{h}_{q,N}]$. As shown in Fig. 3, $k \in \{1, 2, \dots, N-1\}$ is the index of the k th block diagonal above the main block diagonal (whose index $k = 0$) of \mathbf{M}_q , while $k \in \{-(N-1), \dots, -2, -1\}$ is the index of the $|k|$ th block diagonal below the main block diagonal. Given a certain k , $\mathbf{M}_{q,k}$ is generated by retaining the k th block diagonal of \mathbf{M}_q but setting all the other blocks as zero matrices. For $k \neq 0$, the non-Hermitian matrix $\mathbf{M}_{q,-k} = \mathbf{M}_{q,k}^H$, while $\mathbf{M}_{q,0} \succeq 0$. Thus, $v_{out,q}$ can be rewritten as

$$v_{out,q} = \frac{1}{2} \beta_2 \mathbf{s}^H \mathbf{M}_{q,0} \mathbf{s} + \frac{3}{8} \beta_4 \mathbf{s}^H \mathbf{M}_{q,0} \mathbf{s} (\mathbf{s}^H \mathbf{M}_{q,0} \mathbf{s})^H + \frac{3}{4} \beta_4 \sum_{k=1}^{N-1} \mathbf{s}^H \mathbf{M}_{q,k} \mathbf{s} (\mathbf{s}^H \mathbf{M}_{q,k} \mathbf{s})^H. \quad (9)$$

The output DC power of all rectifiers are combined together by a DC combining circuit such as MIMO switching DC-DC converter [30] as shown in Fig. 2. The total output DC power is then given by $P_{out} = \sum_{q=1}^Q v_{out,q}^2 / R_L$ where we assume each rectifier has the same load R_L . Therefore, we aim to maximize the total output DC power subject to the transmit power constraint, which can be formulated as

$$\max_{\mathbf{s}} \left\{ \sum_{q=1}^Q \frac{v_{out,q}^2}{R_L} : \frac{1}{2} \|\mathbf{s}\|^2 \leq P \right\}. \quad (10)$$

The objective function (10) is an octic polynomial, which in general makes problems (10) NP-hard. To tackle the octic polynomial, auxiliary variables $t_{q,k} = \mathbf{s}^H \mathbf{M}_{q,k} \mathbf{s}$, for $q = 1, \dots, Q$ and $k = 0, \dots, N-1$, are introduced so that the octic objective function (10) can be reduced to quartic polynomial and $v_{out,q}$ can be rewritten as

$$v_{out,q} = \frac{1}{2} \beta_2 t_{q,0} + \frac{3}{8} \beta_4 t_{q,0} t_{q,0}^* + \frac{3}{4} \beta_4 \sum_{k=1}^{N-1} t_{q,k} t_{q,k}^*, \quad (11)$$

which can be further expressed in a more compact form as $v_{out,q} = \frac{1}{2} \beta_2 t_{q,0} + \mathbf{t}_q^H \mathbf{A}_0 \mathbf{t}_q$ with $\mathbf{t}_q = [t_{q,0}, t_{q,1}, \dots, t_{q,N-1}]^T$ and $\mathbf{A}_0 = \text{diag}\{\frac{3}{8}\beta_4, \frac{3}{4}\beta_4, \dots, \frac{3}{4}\beta_4\} \succeq 0$. However, for $k \neq 0$, $\mathbf{M}_{q,k}$ is not Hermitian so that the term $\mathbf{s}^H \mathbf{M}_{q,k} \mathbf{s}$ is essentially a bilinear function, which may also lead to a NP-hard problem. To address this, we introduce an auxiliary rank-1 positive semidefinite matrix variable $\mathbf{X} = \mathbf{s} \mathbf{s}^H$ to linearize the term such that $t_{q,k} = \text{Tr}(\mathbf{M}_{q,k} \mathbf{X})$ for $q = 1, \dots, Q$ and $k = 0, \dots, N-1$. Therefore, we can equivalently rewrite the problem (10) as

$$\max_{t_{q,k}, \mathbf{X} \succeq 0} \sum_{q=1}^Q v_{out,q}^2 \quad (12)$$

$$\text{s.t. } t_{q,k} = \text{Tr}(\mathbf{M}_{q,k} \mathbf{X}), \forall q, k, \quad (13)$$

$$\text{Tr}(\mathbf{X}) \leq 2P, \quad (14)$$

$$\text{rank}(\mathbf{X}) = 1. \quad (15)$$

The rank constraint (15), however, makes the problem (12)-(15) NP-hard in general. To handle this, we use SDR to relax the rank constraint (15) and then solve the relaxed problem (12)-(14). $v_{out,q}$ is convex with respect to $t_{q,k}$ and $v_{out,q} \geq 0$, so the objective function $\sum_{q=1}^Q v_{out,q}^2$ is convex with respect to $t_{q,k}$ according to the compositions rules [31]. Therefore, the relaxed problem (12)-(14) is essentially maximizing a convex function subject to convex constraints, but unfortunately it is still not a convex problem.

To solve the nonconvex relaxed problem (12)-(14), we use SCA to approximate the convex objective function as a linear function and iteratively solve the approximated problem. Particularly, at iteration i , the convex objective function $\sum_{q=1}^Q v_{out,q}^2$ is approximated at $\mathbf{t}_q^{(i-1)}$, which is the optimal \mathbf{t}_q solved at iteration $(i-1)$, as a linear function by its first-order Taylor expansion [32], so that we have

$$\sum_{q=1}^Q v_{out,q}^2 \geq \sum_{q=1}^Q v_{out,q}^{(i-1)} \left(\beta_2 t_{q,0} + 4\Re \left\{ \mathbf{t}_q^{(i-1)H} \mathbf{A}_0 \mathbf{t}_q \right\} \right) - \sum_{q=1}^Q v_{out,q}^{(i-1)} \left(v_{out,q}^{(i-1)} + 2\mathbf{t}_q^{(i-1)H} \mathbf{A}_0 \mathbf{t}_q^{(i-1)} \right), \quad (16)$$

where the right hand side is the linear approximated objective function with $v_{out,q}^{(i-1)} = \frac{1}{2} \beta_2 t_{q,0}^{(i-1)} + \mathbf{t}_q^{(i-1)H} \mathbf{A}_0 \mathbf{t}_q^{(i-1)}$. Then, ignoring the constant in the linear approximated objective

function, we can equivalently formulate the approximate problem (AP) at iteration i as

$$\max_{\mathbf{t}_{q,k}, \mathbf{X} \succeq \mathbf{0}} \sum_{q=1}^Q v_{\text{out},q}^{(i-1)} \left(\beta_2 t_{q,0} + 4\Re \left\{ \mathbf{t}_q^{(i-1)H} \mathbf{A}_0 \mathbf{t}_q \right\} \right) \quad (17)$$

$$\text{s.t.} \quad t_{q,k} = \text{Tr}(\mathbf{M}_{q,k} \mathbf{X}), \quad \forall q, k, \quad (18)$$

$$\text{Tr}(\mathbf{X}) \leq 2P, \quad (19)$$

which is a Semidefinite Programming (SDP). Substituting (18) into (17), we can rewrite the problem (17)-(19) in an equivalent compact form as

$$\max_{\mathbf{X} \succeq \mathbf{0}} \{ \text{Tr}(\mathbf{A}_1 \mathbf{X}) : \text{Tr}(\mathbf{X}) \leq 2P \}, \quad (20)$$

where $\mathbf{A}_1 = \mathbf{C}_1 + \mathbf{C}_1^H$ is Hermitian and \mathbf{C}_1 is given by

$$\mathbf{C}_1 = \sum_{q=1}^Q v_{\text{out},q}^{(i-1)} \left(\frac{2\beta_2 + 3\beta_4 t_{q,0}^{(i-1)}}{4} \mathbf{M}_{q,0} + \frac{3}{2} \beta_4 \sum_{k=1}^{N-1} t_{q,k}^{(i-1)*} \mathbf{M}_{q,k} \right). \quad (21)$$

According to [7], [33], the problem (20) has a rank-1 global optimal solution \mathbf{X}^* given by

$$\mathbf{X}^* = \mathbf{s}^* \mathbf{s}^{*H}, \quad (22)$$

$$\mathbf{s}^* = \sqrt{2P} [\mathbf{U}_{\mathbf{A}_1}]_{\max}, \quad (23)$$

where $[\mathbf{U}_{\mathbf{A}_1}]_{\max}$ is the eigenvector of \mathbf{A}_1 corresponding to the maximum eigenvalue. Therefore, at each iteration, we perform Eigenvalue Decomposition (EVD) for \mathbf{A}_1 by the QR algorithm [34] with a computational complexity of $\mathcal{O}(M^3 N^3)$ to find a rank-1 global optimal solution of the AP (17)-(19), and we repeat the iterations till convergence. The SCA guarantees to converge to a stationary point of the relaxed problem (12)-(14). In addition, because such stationary point is guaranteed to be rank-1 (achieved by (22) and (23)), it is also a stationary point of the original problem (12)-(15). The initialization of the SCA is important and affects the convergence speed. Specifically, using singular value decomposition (SVD), we decompose the channel matrix as $\mathbf{H}_n = \mathbf{U}_n \mathbf{\Sigma}_n \mathbf{V}_n^H$ where \mathbf{U}_n is a $Q \times Q$ unitary matrix, \mathbf{V}_n is a $M \times M$ unitary matrix, and $\mathbf{\Sigma}_n$ is a $Q \times M$ diagonal matrix. We choose a good initial point as $\mathbf{s}_n^{(0)} = \sigma_n \sqrt{2P / \sum_{n=1}^N \sigma_n^2} [\mathbf{V}_n]_{\max}$ where σ_n is the maximum singular value of \mathbf{H}_n and $[\mathbf{V}_n]_{\max}$ is the vector in \mathbf{V}_n corresponding to σ_n . Accordingly, we have that $\mathbf{s}^{(0)} = [\mathbf{s}_1^{(0)T}, \mathbf{s}_2^{(0)T}, \dots, \mathbf{s}_N^{(0)T}]^T$, $\mathbf{X}^{(0)} = \mathbf{s}^{(0)} \mathbf{s}^{(0)H}$, $t_{q,k}^{(0)} = \text{Tr}(\mathbf{M}_{q,k} \mathbf{X}^{(0)})$, and $v_{\text{out},q}^{(0)} = \frac{1}{2} \beta_2 t_{q,0}^{(0)} + \mathbf{t}_q^{(0)H} \mathbf{A}_0 \mathbf{t}_q^{(0)}$.

Algorithm 1 summarizes the overall algorithm for jointly optimizing the waveform and beamforming with DC combin-

Algorithm 1 Joint Waveform and Beamforming Optimization with DC Combining.

- 1) **Initialize:** $i = 0$, $\mathbf{s}^{(0)}$, $\mathbf{X}^{(0)}$, $\mathbf{t}_q^{(0)}$, and $v_{\text{out},q}^{(0)}$ for $\forall q$;
 - 2) **do**
 - 3) $i = i + 1$;
 - 4) $\mathbf{A}_1 = \mathbf{C}_1 + \mathbf{C}_1^H$ where \mathbf{C}_1 is computed by (21);
 - 5) Update $\mathbf{s}^{(i)} = \sqrt{2P} [\mathbf{U}_{\mathbf{A}_1}]_{\max}$; $\mathbf{X}^{(i)} = \mathbf{s}^{(i)} \mathbf{s}^{(i)H}$;
 - 6) Update $t_{q,k}^{(i)} = \text{Tr}(\mathbf{M}_{q,k} \mathbf{X}^{(i)})$, $\forall q, k$;
 - 7) Update $v_{\text{out},q}^{(i)} = \frac{1}{2} \beta_2 t_{q,0}^{(i)} + \mathbf{t}_q^{(i)H} \mathbf{A}_0 \mathbf{t}_q^{(i)}$, $\forall q$;
 - 8) **until** $\|\mathbf{s}^{(i)} - \mathbf{s}^{(i-1)}\| / \|\mathbf{s}^{(i)}\| \leq \epsilon$ or $i = i_{\max}$
 - 9) Set $\mathbf{s}^* = \mathbf{s}^{(i)}$;
-

ing². It solves a stationary point of the problem (10).

V. JOINT WAVEFORM AND BEAMFORMING OPTIMIZATION WITH RF COMBINING

Consider the RF combining scheme for the multiple antennas as shown in Fig. 4. All receive antennas are connected to an RF combining circuit such as an RF power combiner. The received signals at all receive antennas are combined together so that the RF combined signal $\tilde{y}(t)$ can be expressed as

$$\tilde{y}(t) = \Re \left\{ \sum_{n=1}^N \mathbf{w}_n^H \mathbf{H}_n \mathbf{s}_n e^{j\omega_n t} \right\}, \quad (24)$$

where \mathbf{w}_n denotes the receive beamformer at the n th angular frequency. Using the nonlinear rectenna model (5) with the truncation order $n_0 = 4$, the output DC voltage is given by

$$v_{\text{out}} = \beta_2 \mathcal{E} \left\{ \tilde{y}(t)^2 \right\} + \beta_4 \mathcal{E} \left\{ \tilde{y}(t)^4 \right\}, \quad (25)$$

where $\mathcal{E} \left\{ \tilde{y}(t)^2 \right\}$ and $\mathcal{E} \left\{ \tilde{y}(t)^4 \right\}$ are given by

$$\mathcal{E} \left\{ \tilde{y}(t)^2 \right\} = \frac{1}{2} \sum_{n=1}^N \mathbf{s}_n^H \mathbf{H}_n^H \mathbf{w}_n \mathbf{w}_n^H \mathbf{H}_n \mathbf{s}_n \quad (26)$$

$$\mathcal{E} \left\{ \tilde{y}(t)^4 \right\} = \frac{3}{8} \sum_{\substack{n_1, n_2, n_3, n_4 \\ n_1 + n_2 = n_3 + n_4}} \left(\mathbf{s}_{n_3}^H \mathbf{H}_{n_3}^H \mathbf{w}_{n_3} \mathbf{w}_{n_1}^H \mathbf{H}_{n_1} \mathbf{s}_{n_1} \cdot \mathbf{s}_{n_4}^H \mathbf{H}_{n_4}^H \mathbf{w}_{n_4} \mathbf{w}_{n_2}^H \mathbf{H}_{n_2} \mathbf{s}_{n_2} \right). \quad (27)$$

²Algorithm 1 proposed in this paper is different from the algorithm for beamforming only design with DC combining in [27] in three aspects: 1) The algorithm in [27] cannot theoretically guarantee finding a stationary point, but Algorithm 1 can; 2) The algorithm in [27] is only for a continuous sinewave, but Algorithm 1 is for multi-sine wave which is more general and challenging to optimize; 3) In each iteration, the algorithm in [27] needs to solve a convex problem but Algorithm 1 only needs to perform EVD which has lower computation complexity. In addition, Algorithm 1 proposed in this paper is different from Algorithm 2 in [7] in three aspects: 1) The objective function optimized by Algorithm 1 is the total output DC power $\sum_{q=1}^Q v_{\text{out},q}^2 / R_L$ in single user MIMO WPT systems, which is an octic polynomial of \mathbf{s} . However, the objective function optimized by Algorithm 2 in [7] is the weighted sum output DC voltage $\sum_{q=1}^Q w_q v_{\text{out},q}$ in multi-user MISO WPT systems, which is a quartic polynomial of \mathbf{s} ; 2) Algorithm 1 uses SCA to approximate $\sum_{q=1}^Q v_{\text{out},q}^2 / R_L$ as a linear function of \mathbf{t}_q while Algorithm 2 in [7] uses SCA to approximate $\sum_{q=1}^Q w_q v_{\text{out},q}$ as a linear function; 3) Algorithm 1 considers $v_{\text{out},q}^{(i-1)}$ at iteration i but Algorithm 2 in [7] does not consider $v_{\text{out},q}^{(i-1)}$. The matrix \mathbf{A}_1 in Algorithm 1 has a different definition from the matrix $\hat{\mathbf{A}}_1$ in Algorithm 2 in [7].

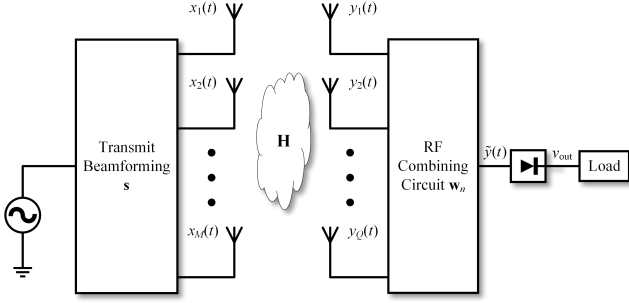


Fig. 4. Schematic of the multi-sine MIMO WPT system with RF combining in the receiver.

A. General Receive Beamforming

We first consider an RF combining scheme with general receive beamforming satisfying the constraint that $\|\mathbf{w}_n\| \leq 1 \forall n$. This constraint results from the fact that the output power of the passive RF combining circuit should be equal or less than the input power [27].

We aim to maximize the total output DC power subject to the transmit power constraint and the general receive beamforming constraint. Maximizing the output DC power $P_{\text{out}} = v_{\text{out}}^2/R_L$ is equivalent to maximizing v_{out} , so we can formulate the equivalent problem as

$$\max_{\mathbf{s}, \mathbf{w}_n} \left\{ v_{\text{out}} : \frac{1}{2} \|\mathbf{s}\|^2 \leq P, \|\mathbf{w}_n\| \leq 1, \forall n \right\}. \quad (28)$$

To handle this, we introduce an auxiliary multiple-input single-output (MISO) channel $\tilde{\mathbf{h}}_n = \mathbf{w}_n^H \mathbf{H}_n \forall n$, which is an effective MISO channel obtained by concatenating the MIMO channel \mathbf{H}_n with the RF combining \mathbf{w}_n . For the joint beamforming and waveform optimization in the equivalent multi-sine MISO WPT system, it is shown in [6] and [7] that the optimal \mathbf{s}_n is actually a matched beamformer of the form

$$\mathbf{s}_n = \xi_n \frac{\tilde{\mathbf{h}}_n^H}{\|\tilde{\mathbf{h}}_n\|} = \xi_n \frac{(\mathbf{w}_n^H \mathbf{H}_n)^H}{\|\mathbf{w}_n^H \mathbf{H}_n\|}, \quad (29)$$

where $\xi_n > 0$ without loss of generality and ξ_n^2 denotes the power allocated to the sinewave at the n th angular frequency. We group all ξ_n into a vector $\mathbf{p} = [\xi_1, \xi_2, \dots, \xi_N]^T$ such that \mathbf{p} describes the power allocation to the different sinewaves and $\frac{1}{2} \|\mathbf{p}\|^2 \leq P$. With the optimal \mathbf{s}_n (29), the problem (28) can be equivalently converted to the following problem

$$\max_{\mathbf{p}, \mathbf{w}_n} \left\{ v_{\text{out}} : \frac{1}{2} \|\mathbf{p}\|^2 \leq P, \|\mathbf{w}_n\| \leq 1, \forall n \right\}, \quad (30)$$

where the terms $\mathcal{E} \left\{ \tilde{y}(t)^2 \right\}$ and $\mathcal{E} \left\{ \tilde{y}(t)^4 \right\}$ in the objective function (30) can be achieved by substituting (29) into (26) and (27), i.e.

$$\mathcal{E} \left\{ \tilde{y}(t)^2 \right\} = \frac{1}{2} \left[\sum_{n=1}^N \|\tilde{\mathbf{h}}_n\|^2 \xi_n^2 \right], \quad (31)$$

$$\mathcal{E} \left\{ \tilde{y}(t)^4 \right\} = \frac{3}{8} \left[\sum_{\substack{n_1, n_2, n_3, n_4 \\ n_1 + n_2 = n_3 + n_4}} \left[\prod_{j=1}^4 \|\tilde{\mathbf{h}}_{n_j}\| \xi_{n_j} \right] \right]. \quad (32)$$

From (31) and (32), we can find that v_{out} increases with $\|\tilde{\mathbf{h}}_n\|$ given any ξ_n . Therefore, the optimal receive beamformer \mathbf{w}_n^* maximizing the output DC power is given by $\mathbf{w}_n^* = \operatorname{argmax}_{\|\mathbf{w}_n\| \leq 1} \|\tilde{\mathbf{h}}_n\|$. A closed form solution for \mathbf{w}_n^* can be obtained by using SVD $\mathbf{H}_n = \mathbf{U}_n \Sigma_n \mathbf{V}_n^H$. Then, the optimal receive beamformer \mathbf{w}_n^* is given by

$$\mathbf{w}_n^* = [\mathbf{U}_n]_{\max}, \quad (33)$$

where $[\mathbf{U}_n]_{\max}$ refers to the vector in \mathbf{U}_n corresponding to σ_n which is the maximum singular value of \mathbf{H}_n . Therefore, the maximum value of $\|\tilde{\mathbf{h}}_n\|$ is σ_n .

With the optimal \mathbf{s}_n (29) and the optimal receive beamformer \mathbf{w}_n^* (33), the joint waveform and beamforming optimization for the multi-sine MIMO WPT system with the general receive beamforming can be equivalently converted to the waveform optimization for the multi-sine single-input single-output (SISO) WPT system. Namely, the problem (30) is equivalent to

$$\max_{\mathbf{p}} \left\{ v_{\text{out}} : \frac{1}{2} \|\mathbf{p}\|^2 \leq P \right\}, \quad (34)$$

which finds the optimal power allocation across sinewaves to maximize the output DC voltage. The terms $\mathcal{E} \left\{ \tilde{y}(t)^2 \right\}$ and $\mathcal{E} \left\{ \tilde{y}(t)^4 \right\}$ in the objective function (34) are given by

$$\mathcal{E} \left\{ \tilde{y}(t)^2 \right\} = \frac{1}{2} \left[\sum_{n=1}^N \sigma_n^2 \xi_n^2 \right], \quad (35)$$

$$\mathcal{E} \left\{ \tilde{y}(t)^4 \right\} = \frac{3}{8} \left[\sum_{\substack{n_1, n_2, n_3, n_4 \\ n_1 + n_2 = n_3 + n_4}} \left[\prod_{j=1}^4 \sigma_{n_j} \xi_{n_j} \right] \right]. \quad (36)$$

Leveraging (35) and (36), the objective function v_{out} in (34) writes as a posynomial, and can be written in the compact form $v_{\text{out}} = \sum_{k=1}^K g_k(\mathbf{p})$ where K denotes the number of monomials in the posynomial and $g_k(\mathbf{p})$ denotes the k th monomial. $g_k(\mathbf{p})$ can be defined as follows. We first exhaustively search $n_1 = 1, \dots, N$, $n_2 = 1, \dots, N$, $n_3 = 1, \dots, N$, and $n_4 = 1, \dots, N$ to find all the combinations of n_1, n_2, n_3, n_4 which satisfy $n_1 + n_2 = n_3 + n_4$. We denote the k th combination of n_1, n_2, n_3, n_4 satisfying $n_1 + n_2 = n_3 + n_4$ as $n_1^{(k)}, n_2^{(k)}, n_3^{(k)}, n_4^{(k)}$, and there are in total \bar{K} such combinations. Therefore, we can define $g_k(\mathbf{p})$ as

$$g_k(\mathbf{p}) = \begin{cases} \frac{3\beta_4}{8} \prod_{j=1}^4 \sigma_{n_j^{(k)}} \xi_{n_j^{(k)}} & , k = 1, \dots, \bar{K} \\ \frac{\beta_2}{2} \sigma_{k-\bar{K}}^2 \xi_{k-\bar{K}}^2 & , k = \bar{K} + 1, \dots, \bar{K} + N \end{cases} \quad (37)$$

so that we can write $v_{\text{out}} = \sum_{k=1}^K g_k(\mathbf{p})$ where $K = \bar{K} + N$. The problem (34) aims to maximize a posynomial subject to a power constraint (the power is also a posynomial), which is not a standard Geometric Programming (GP). To handle this,

Algorithm 2 Joint Waveform and Beamforming Optimization with RF Combining using General Receive Beamforming.

- 1) **Initialize:** $i = 0$ and $\mathbf{p}^{(0)}$;
 - 2) **do**
 - 3) $i = i + 1$;
 - 4) $\gamma_k = g_k(\mathbf{p}^{(i-1)}) / \sum_{k=1}^K g_k(\mathbf{p}^{(i-1)})$, $\forall k$;
 - 5) Update $\mathbf{p}^{(i)}$ by solving GP (42)-(44);
 - 6) **until** $\|\mathbf{p}^{(i)} - \mathbf{p}^{(i-1)}\| / \|\mathbf{p}^{(i)}\| \leq \epsilon$ or $i = i_{\max}$
 - 7) Set $\mathbf{p}^* = [\xi_1^*, \xi_2^*, \dots, \xi_N^*]^T = \mathbf{p}^{(i)}$;
 - 8) Set $\mathbf{w}_n^* = [\mathbf{U}_n]_{\max}$, $\forall n$;
 - 9) Set $\mathbf{s}_n^* = \xi_n^* \frac{\mathbf{w}_n^{*H} \mathbf{H}_n}{\|\mathbf{w}_n^{*H} \mathbf{H}_n\|}$, $\forall n$;
-

we introduce an auxiliary variable $\zeta_0 > 0$ and equivalently rewrite the problem (34) as

$$\min_{\mathbf{p}, \zeta_0} \frac{1}{\zeta_0} \quad (38)$$

$$\text{s.t.} \quad \frac{1}{2} \|\mathbf{p}\|^2 \leq P, \quad (39)$$

$$\frac{\zeta_0}{\sum_{k=1}^K g_k(\mathbf{p})} \leq 1. \quad (40)$$

However, $\zeta_0 / \sum_{k=1}^K g_k(\mathbf{p})$ is not a posynomial, which prevents the use of standard GP tools. Therefore, we use SCA to approximate $\zeta_0 / \sum_{k=1}^K g_k(\mathbf{p})$ as a monomial and iteratively solve the approximated problem. Particularly, at iteration i , $\zeta_0 / \sum_{k=1}^K g_k(\mathbf{p})$ is approximated at $\mathbf{p}^{(i-1)}$, which is the optimal \mathbf{p} solved at iteration $(i-1)$, as a monomial based on the fact that an arithmetic mean (AM) is greater or equal to the geometric mean (GM) [35], so we have

$$\frac{\zeta_0}{\sum_{k=1}^K g_k(\mathbf{p})} \leq \frac{\zeta_0}{\prod_{k=1}^K \left(\frac{g_k(\mathbf{p})}{\gamma_k} \right)^{\gamma_k}}, \quad (41)$$

where $\gamma_k = g_k(\mathbf{p}^{(i-1)}) / \sum_{k=1}^K g_k(\mathbf{p}^{(i-1)}) > 0$ and $\sum_{k=1}^K \gamma_k = 1$. We replace the constraint $\zeta_0 / \sum_{k=1}^K g_k(\mathbf{p}) \leq 1$ with $\zeta_0 \prod_{k=1}^K \left(\frac{g_k(\mathbf{p})}{\gamma_k} \right)^{-\gamma_k} \leq 1$ in a conservative way and then the problem (38)-(40) can be approximated as a standard GP

$$\min_{\mathbf{p}, \zeta_0} \frac{1}{\zeta_0} \quad (42)$$

$$\text{s.t.} \quad \frac{1}{2} \|\mathbf{p}\|^2 \leq P, \quad (43)$$

$$\zeta_0 \prod_{k=1}^K \left(\frac{g_k(\mathbf{p})}{\gamma_k} \right)^{-\gamma_k} \leq 1, \quad (44)$$

which can be solved by existing software using interior point methods, e.g. CVX [36]. Therefore, at each iteration of SCA, we solve the standard GP (42)-(44) for an updated set of $\{\gamma_k\}$ by using interior point methods which have provably polynomial time complexity [35], and we repeat the iterations till convergence. The SCA guarantees to converge to a stationary point of the problem (38)-(40) [35]. Let \mathbf{p}^* denotes the stationary point of the problem (38)-(40). Given the optimal \mathbf{w}_n^* (33) and \mathbf{p}^* , the optimal \mathbf{s}_n^* can be found by (29). The initialization of the SCA is important and affects the

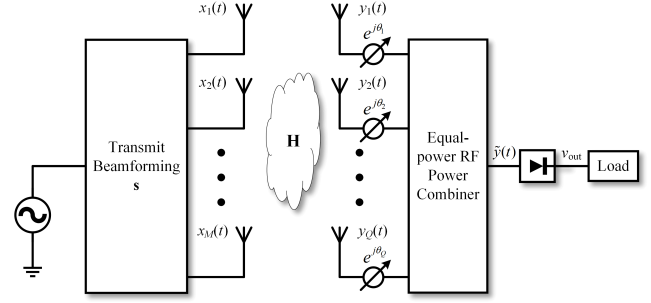


Fig. 5. Schematic of the multi-sine MIMO WPT system with RF combining using analog receive beamforming in the receiver.

convergence speed. Herein, we choose a good initial point for the SCA as $\mathbf{p}^{(0)} = \sqrt{2P / \sum_{n=1}^N \sigma_n^2} [\sigma_1, \sigma_2, \dots, \sigma_N]^T$.

Algorithm 2 summarizes the overall algorithm for jointly optimizing the waveform and beamforming with RF combining using general receive beamforming³. It solves a stationary point of the problem (28).

B. Analog Receive Beamforming

We also consider an RF combining scheme using a practical RF combining circuit as shown in Fig. 5. We refer to it as analog receive beamforming. It consists of an equal-power RF power combiner and Q phase shifters. Each receive antenna is connected to a phase shifter and the outputs of the Q phase shifters are connected to the RF power combiner. Phase shifters have been widely used in hybrid precoding for massive MIMO communications and the phase shifts for multiple carrier frequencies are usually modeled to be identical [37], [38]. Therefore, the analog receive beamformers for the N sinewaves can be modeled to be identical, i.e.

$$\mathbf{w}_n = \frac{1}{\sqrt{Q}} [e^{-j\theta_1}, e^{-j\theta_2}, \dots, e^{-j\theta_Q}]^T, \quad \forall n, \quad (45)$$

$$-\pi \leq \theta_q < \pi, \quad \forall q, \quad (46)$$

where θ_q denotes the q th phase shift for $q = 1, \dots, Q$.

We aim to maximize the output DC voltage v_{out} (equivalently maximize the output DC power) subject to the transmit power constraint and the analog receive beamforming constraints (45) and (46), so we can formulate the problem as

$$\max_{\mathbf{s}, \mathbf{w}_n, \theta_q} v_{\text{out}} \quad (47)$$

$$\text{s.t.} \quad \frac{1}{2} \|\mathbf{s}\|^2 \leq P, \quad (48)$$

$$\mathbf{w}_n = \frac{1}{\sqrt{Q}} [e^{-j\theta_1}, e^{-j\theta_2}, \dots, e^{-j\theta_Q}]^T, \quad \forall n, \quad (49)$$

$$-\pi \leq \theta_q < \pi, \quad \forall q, \quad (50)$$

where v_{out} is given by (25), (26), and (27). The constraints (49) and (50) are more restrictive than the general receive

³In beamforming only design [27], the general receive beamforming has a simple closed form solution but only valid for a continuous sinewave. However, when it comes to joint waveform and beamforming design, the optimization is more challenging as the waveform needs to be particularly optimized. Therefore we propose Algorithms 2 in this paper for more general multi-sine wave to increase the output DC power.

beamforming constraint $\|\mathbf{w}_n\| \leq 1 \forall n$, so the analog receive beamforming provides a lower output DC voltage than the general receive beamforming.

The problem (47)-(50) can be simplified in three steps: 1) introducing auxiliary MISO channels $\tilde{\mathbf{h}}_n = \mathbf{w}_n^H \mathbf{H}_n \forall n$ so that the optimal \mathbf{s}_n is provided by (29) as shown in [6] and [7]; 2) introducing an auxiliary variable $\mathbf{w} = \mathbf{w}_n \forall n$ so that the constraints (49) and (50) are equivalent to $|\mathbf{w}_q| = \frac{1}{\sqrt{Q}} \forall q$; and 3) introducing auxiliary variables $r_n = \|\tilde{\mathbf{h}}_n\| = \|\mathbf{w}^H \mathbf{H}_n\| > 0 \forall n$. Hence we can equivalently simplify problem (47)-(50) as

$$\max_{\mathbf{p}, \mathbf{w}, r_n} v_{\text{out}} \quad (51)$$

$$\text{s.t.} \quad \frac{1}{2} \|\mathbf{p}\|^2 \leq P, \quad (52)$$

$$|\mathbf{w}_q| = \frac{1}{\sqrt{Q}}, \forall q, \quad (53)$$

$$r_n^2 = \mathbf{w}^H \mathbf{H}_n \mathbf{H}_n^H \mathbf{w}, \forall n, \quad (54)$$

where the terms $\mathcal{E}\{\tilde{y}(t)^2\}$ and $\mathcal{E}\{\tilde{y}(t)^4\}$ in the objective function (51) are given by

$$\mathcal{E}\{\tilde{y}(t)^2\} = \frac{1}{2} \left[\sum_{n=1}^N r_n^2 \xi_n^2 \right], \quad (55)$$

$$\mathcal{E}\{\tilde{y}(t)^4\} = \frac{3}{8} \left[\sum_{\substack{n_1, n_2, n_3, n_4 \\ n_1+n_2=n_3+n_4}} \left[\prod_{j=1}^4 r_{n_j} \xi_{n_j} \right] \right]. \quad (56)$$

Leveraging (55) and (56), the objective function v_{out} (51) is a posynomial so that it can be written in a compact form that $v_{\text{out}} = \sum_{k=1}^{K'} g'_k(\mathbf{p}, \mathbf{r})$ where K' denotes the number of monomials in the posynomial and $g'_k(\mathbf{p}, \mathbf{r})$ denotes the k th monomial with $\mathbf{r} = [r_1, r_2, \dots, r_N]^T$. $g'_k(\mathbf{p}, \mathbf{r})$ can be defined in a similar way to (37). The problem (51)-(54) is more difficult than the problem (30) (the general receive beamforming) because we cannot decouple the optimization of \mathbf{p} and \mathbf{w} to provide a closed-form solution for the optimal \mathbf{w} . Therefore, we need to jointly optimize \mathbf{p} and \mathbf{w} . To that end, we first replace the constraint $|\mathbf{w}_q| = \frac{1}{\sqrt{Q}}$ with $|\mathbf{w}_q| \leq \frac{1}{\sqrt{Q}}$ without affecting the optimal solution of the problem (51)-(54). The reason is that the objective function (51) monotonically increases with r_n and $r_n = \|\mathbf{w}^H \mathbf{H}_n\|$. Hence, the optimal \mathbf{w} that maximizes the objective function must satisfy the equality even though $|\mathbf{w}_q| \leq \frac{1}{\sqrt{Q}}$. We also replace the constraint $r_n^2 = \mathbf{w}^H \mathbf{H}_n \mathbf{H}_n^H \mathbf{w}$ with $r_n^2 \leq \mathbf{w}^H \mathbf{H}_n \mathbf{H}_n^H \mathbf{w}$ without affecting the optimal solution of the problem (51)-(54) since the objective function (51) monotonically increases with r_n . Hence, the optimal r_n that maximizes the objective function must satisfy the equality even though $r_n^2 \leq \mathbf{w}^H \mathbf{H}_n \mathbf{H}_n^H \mathbf{w}$. In addition, we introduce an auxiliary variable $\zeta_1 > 0$ and then equivalently rewrite the

problem (51)-(54) as

$$\min_{\mathbf{p}, \mathbf{w}, r_n, \zeta_1} \frac{1}{\zeta_1} \quad (57)$$

$$\text{s.t.} \quad \frac{1}{2} \|\mathbf{p}\|^2 \leq P, \quad (58)$$

$$|\mathbf{w}_q| \leq \frac{1}{\sqrt{Q}}, \forall q, \quad (59)$$

$$r_n^2 \leq \mathbf{w}^H \mathbf{H}_n \mathbf{H}_n^H \mathbf{w}, \forall n, \quad (60)$$

$$\frac{\zeta_1}{\sum_{k=1}^{K'} g'_k(\mathbf{p}, \mathbf{r})} \leq 1. \quad (61)$$

However, (60) is not convex, and $\zeta_1 / \sum_{k=1}^{K'} g'_k(\mathbf{p}, \mathbf{r})$ is not a posynomial which prevents the transformation to a convex constraint.

To solve the nonconvex problem (57)-(61), we use SCA to approximate (60) and (61) as convex constraints and iteratively solve the approximated problem. Particularly, at iteration i , $r_n^2 \leq \mathbf{w}^H \mathbf{H}_n \mathbf{H}_n^H \mathbf{w} \forall n$ is approximated at $\mathbf{w}^{(i-1)}$, which is the optimal \mathbf{w} solved at iteration $(i-1)$, as a convex constraint

$$r_n^2 \leq 2\Re \left\{ \mathbf{w}^{(i-1)H} \mathbf{H}_n \mathbf{H}_n^H \mathbf{w} \right\} - \mathbf{w}^{(i-1)H} \mathbf{H}_n \mathbf{H}_n^H \mathbf{w}^{(i-1)}, \forall n, \quad (62)$$

based on the first-order Taylor expansion [32], while $\zeta_1 / \sum_{k=1}^{K'} g'_k(\mathbf{p}, \mathbf{r})$ is approximated at $\mathbf{p}^{(i-1)}$ and $\mathbf{r}^{(i-1)}$, which is optimal \mathbf{p} and \mathbf{r} solved at iteration $(i-1)$, as a monomial based on the AM-GM inequality [35], i.e.

$$\frac{\zeta_1}{\sum_{k=1}^{K'} g'_k(\mathbf{p}, \mathbf{r})} \leq \frac{\zeta_1}{\prod_{k=1}^{K'} \left(\frac{g'_k(\mathbf{p}, \mathbf{r})}{\gamma'_k} \right)^{\gamma'_k}}, \quad (63)$$

where $\gamma'_k = g'_k(\mathbf{p}^{(i-1)}, \mathbf{r}^{(i-1)}) / \sum_{k=1}^{K'} g'_k(\mathbf{p}^{(i-1)}, \mathbf{r}^{(i-1)}) \forall k$ and $\sum_{k=1}^{K'} \gamma'_k = 1$. We replace (60) with (62) and replace (61) with $\zeta_1 \prod_{k=1}^{K'} \left(\frac{g'_k(\mathbf{p}, \mathbf{r})}{\gamma'_k} \right)^{-\gamma'_k} \leq 1$ both in a conservative way, so that the problem (57)-(61) can be approximated as

$$\min_{\mathbf{p}, \mathbf{w}, r_n, \zeta_1} \frac{1}{\zeta_1} \quad (64)$$

$$\text{s.t.} \quad \frac{1}{2} \|\mathbf{p}\|^2 \leq P, \quad (65)$$

$$|\mathbf{w}_q| \leq \frac{1}{\sqrt{Q}}, \forall q, \quad (66)$$

$$r_n^2 \leq 2\Re \left\{ \mathbf{w}^{(i-1)H} \mathbf{H}_n \mathbf{H}_n^H \mathbf{w} \right\} - \mathbf{w}^{(i-1)H} \mathbf{H}_n \mathbf{H}_n^H \mathbf{w}^{(i-1)}, \forall n, \quad (67)$$

$$\zeta_1 \prod_{k=1}^{K'} \left(\frac{g'_k(\mathbf{p}, \mathbf{r})}{\gamma'_k} \right)^{-\gamma'_k} \leq 1, \quad (68)$$

which can be equivalently transformed to a convex problem by using a logarithmic transformation. To see the details, we first rewrite the monomial term as $\zeta_1 \prod_{k=1}^{K'} \left(\frac{g'_k(\mathbf{p}, \mathbf{r})}{\gamma'_k} \right)^{-\gamma'_k} = c_1 \zeta_1 \prod_{n=1}^N \xi_n^{a_n} r_n^{b_n}$ where $c_1, a_n, b_n \forall n$ are constants. We then introduce auxiliary variables $\tilde{\zeta}_1 = \log \zeta_1, \tilde{\xi}_n = \log \xi_n, \tilde{r}_n = \log r_n \forall n$, so that $e^{\tilde{\zeta}_1} = \zeta_1, e^{\tilde{\xi}_n} = \xi_n, e^{\tilde{r}_n} = r_n \forall n$. Using the logarithmic transformation for the objective function (64)

Algorithm 3 Joint Waveform and Beamforming Optimization with RF combining using Analog Receive Beamforming.

- 1) **Initialize:** $i = 0$, $\mathbf{p}^{(0)}$, $\mathbf{w}^{(0)}$, $\mathbf{r}^{(0)}$, and $\zeta_1^{(0)}$;
 - 2) **do**
 - 3) $i = i + 1$;
 - 4) $\gamma'_k = g'_k(\mathbf{p}^{(i-1)}, \mathbf{r}^{(i-1)}) / \sum_{k=1}^{K'} g'_k(\mathbf{p}^{(i-1)}, \mathbf{r}^{(i-1)})$;
 - 5) Update $\mathbf{p}^{(i)}$, $\mathbf{w}^{(i)}$, $\mathbf{r}^{(i)}$, $\zeta_1^{(i)}$ by solving (64)-(68);
 - 6) **until** $|\zeta_1^{(i)} - \zeta_1^{(i-1)}| / |\zeta_1^{(i)}| < \epsilon$ or $i = i_{\max}$
 - 7) Set $\mathbf{p}^* = [\zeta_1^*, \zeta_2^*, \dots, \zeta_N^*]^T = \mathbf{p}^{(i)}$;
 - 8) Set $\mathbf{w}^* = \mathbf{w}^{(i)}$;
 - 9) Set $\mathbf{s}_n^* = \zeta_n^* \frac{(\mathbf{w}^{*H} \mathbf{H}_n)^H}{\|\mathbf{w}^{*H} \mathbf{H}_n\|}$, $\forall n$;
-

and the constraints (65), (67), and (68), we can equivalently transform the problem (64)-(68) as

$$\min_{\tilde{\xi}_n, \mathbf{w}, \tilde{r}_n, \tilde{\zeta}_1} -\tilde{\zeta}_1 \quad (69)$$

$$\text{s.t.} \quad \sum_{n=1}^N e^{2\tilde{\xi}_n} \leq 2P, \quad (70)$$

$$|\mathbf{w}_q| \leq \frac{1}{\sqrt{Q}}, \quad \forall q, \quad (71)$$

$$e^{2\tilde{r}_n} \leq 2\Re \left\{ \mathbf{w}^{(i-1)H} \mathbf{H}_n \mathbf{H}_n^H \mathbf{w} \right\} - \mathbf{w}^{(i-1)H} \mathbf{H}_n \mathbf{H}_n^H \mathbf{w}^{(i-1)}, \quad \forall n, \quad (72)$$

$$\log c_1 + \tilde{\zeta}_1 + \sum_{n=1}^N a_n \tilde{\xi}_n + \sum_{n=1}^N b_n \tilde{r}_n \leq 0, \quad (73)$$

which is a convex problem that can be solved by existing software using interior point methods, e.g. CVX. Therefore, at each iteration of SCA, we solve the problem (64)-(68) by solving the equivalent convex problem (69)-(73) with interior point methods which have polynomial time complexity, and we repeat the iteration till convergence. The SCA guarantees to converge to a stationary point of the problem (57)-(61). Let \mathbf{p}^* and \mathbf{w}^* denote the stationary point of the problem (57)-(61). Given \mathbf{p}^* and \mathbf{w}^* , the optimal \mathbf{s}_n^* can be found by (29). The initialization of SCA is important and affects the convergence speed. Herein, we choose a good initial point as $\mathbf{w}^{(0)} = \frac{1}{\sqrt{Q}} e^{j \arg([\mathbf{U}_{\bar{n}}]_{\max})}$ where $\bar{n} = \arg \max_n \sigma_n$ is the strongest channel using SVD $\mathbf{H}_n = \mathbf{U}_n \Sigma_n \mathbf{V}_n^H$ and $[\mathbf{U}_{\bar{n}}]_{\max}$ is the vector in $\mathbf{U}_{\bar{n}}$ corresponding to the maximum singular value of $\mathbf{H}_{\bar{n}}$. Besides $\mathbf{p}^{(0)} = \sqrt{2P / \sum_{n=1}^N \sigma_n^2} [\sigma_1, \sigma_2, \dots, \sigma_N]^T$, $r_n^{(0)} = \|\mathbf{w}^{(0)H} \mathbf{H}_n\|$, and $\zeta_1^{(0)} = 0$.

Algorithm 3 summarizes the overall algorithm for jointly optimizing the waveform and beamforming with RF combining using analog receive beamforming⁴. It solves a stationary point of the problem (47)-(50).

⁴Algorithms 3 proposed in this paper is different from the algorithm for beamforming only design using analog receive beamforming in [27] in two aspects: 1) The algorithm in [27] cannot theoretically guarantee finding a stationary point, but Algorithm 3 can; 2) The algorithm in [27] is only for a continuous sinewave, but Algorithm 3 is for multi-sine wave which is more general and more challenging to optimize.

VI. PERFORMANCE EVALUATIONS

We consider two types of performance evaluations. The first one is based on the simplified and tractable nonlinear rectenna model (5) as introduced in Section III, while the second one relies on an accurate and realistic rectenna modeling in the circuit simulation solver Advanced Design System (ADS).

A. Nonlinear Model-Based Performance Evaluations

The first type of evaluations consider the output DC power averaged over channel realizations of the multi-sine MIMO WPT system with DC and RF combinings. The evaluation is performed in a scenario representative of a WiFi-like environment at a center frequency of 5.18 GHz with a 36 dBm transmit power and 66 dB path loss in a large open space environment with a NLOS channel power delay profile with 18 taps obtained from model B [39]. Taps are modeled as i.i.d. circularly symmetric complex Gaussian random variables, each with an average power ρ_l . The multipath response is normalized such that $\sum_{l=1}^{18} \rho_l = 1$. With one transmit antenna, this leads to an average received power of -30 dBm ($1 \mu\text{W}$). Equivalently, this system model can be viewed as a transmission over the aforementioned normalized multipath channel with an average transmit power fixed to -30 dBm. The N sinewaves are centered around 5.18 GHz with a uniform frequency gap $\Delta\omega = 2\pi\Delta_f$ where $\Delta_f = B/N$ and the bandwidth $B = 10$ MHz. For the parameters of the rectifier, we assume $v_t = 25.86$ mV, $n_i = 1.05$, and $R_L = 10$ k Ω .

For DC combining, we evaluate the adaptive optimized (OPT) waveform and transmit beamforming using Algorithm 1 versus a benchmark: a waveform and transmit beamforming design based on adaptive single sinewave (ASS) strategy [6]. Specifically, we obtain σ_n , which is the maximum singular value of \mathbf{H}_n , by using SVD $\mathbf{H}_n = \mathbf{U}_n \Sigma_n \mathbf{V}_n^H$, and then find the strongest channel $\bar{n} = \arg \max_n \sigma_n$. Therefore, the transmit beamformer $\mathbf{s}_n^{\text{ASS}}$ is given by

$$\mathbf{s}_n^{\text{ASS}} = \begin{cases} \sqrt{2P} [\mathbf{V}_n]_{\max} & , n = \bar{n} \\ \mathbf{0} & , n \neq \bar{n} \end{cases} \quad (74)$$

where $[\mathbf{V}_n]_{\max}$ refers to the vector in \mathbf{V}_n corresponding to the maximum singular value of \mathbf{H}_n . Such transmit beamformer is optimal for maximizing the output DC power when the linear rectenna model (having a constant RF-to-DC conversion efficiency) is considered [40].

For RF combining, we evaluate the adaptive optimized (OPT) waveform and transmit beamforming with the general receive beamforming using Algorithm 2 and the adaptive optimized waveform and transmit beamforming with the analog receive beamforming (ABF) using Algorithm 3. For comparison, we also consider a benchmark: a waveform and transmit beamforming with the general receive beamforming based on ASS strategy. Specifically, we still use SVD for the channel matrix and find the strongest channel $\bar{n} = \arg \max_n \sigma_n$. Therefore, the transmit beamformer $\mathbf{s}_n^{\text{ASS}}$ is given by (74) and the general receive beamformer is given by (33). Interestingly, as shown in [27], RF combining has the same performance as DC combining when the linear rectenna model is considered.

Namely, ASS based RF combining is also optimal considering the linear rectenna model.

Fig. 6 displays the output DC power averaged over channel realizations versus the number of receive antennas Q for different numbers of transmit antennas M and different numbers of frequencies N . We make the following observations.

First, the output DC power increases with the number of transmit antennas and also the number of receive antennas for the five waveform and beamforming designs using DC or RF combinings, showing that the output DC power can be effectively increased by leveraging the transmit or receive beamforming gain.

Second, the output DC power increases with the number of frequencies for the five waveform and beamforming designs using DC or RF combinings. Compared with the beamforming only design ($N = 1$), the jointly waveform and beamforming design ($N > 1$) can provide a higher output DC power, showing the benefit of jointly optimizing the waveform and beamforming over beamforming only. For the ASS based waveform and beamforming, the increase of the output DC power comes from the frequency diversity gain in the frequency selective channel. For the other designs optimized with the nonlinear rectenna model, the increase not only comes from the frequency diversity gain but also the rectenna nonlinearity. Overall, it shows that the output DC power can be effectively increased by leveraging the frequency diversity gain or rectenna nonlinearity through using multi-sine waveform.

Third, for DC combining, the OPT waveform and beamforming achieves higher output DC power than the ASS based waveform and beamforming. This is because the OPT waveform and beamforming leverages the rectenna nonlinearity while the ASS based waveform and beamforming (which is optimized for the inaccurate linear rectenna model) ignores the rectenna nonlinearity. Recall that the rectenna nonlinearity is responsible for the RF-to-DC conversion efficiency to be a function of the input waveform [1], [6]. Ignoring the nonlinearity results in assuming the RF-to-DC conversion efficiency to be constant, which is again demonstrated in this paper to be inaccurate and to lead to suboptimal designs.

Fourth, for RF combining, the OPT general receive beamforming achieves higher output DC power than the ASS based general receive beamforming. Again, this is because the OPT general receive beamforming leverages the rectenna nonlinearity while the ASS based general receiving beamforming ignores the nonlinearity. In addition, the general receive beamforming outperforms the analog receive beamforming. This is because the constraints of the analog receive beamforming (45) and (46) is more restrictive than that of the general receive beamforming.

Fifth, RF combining outperforms DC combining, especially when the number of receive antennas goes large. This is because RF combining leverages the rectenna nonlinearity more efficiently than DC combining. Indeed, the rectenna has a nonlinear characteristics such that the RF-to-DC conversion efficiency increases with the input RF power. RF combining inputs the combined RF signal (having higher RF power) into a single rectifier while DC combining inputs each RF signal to each rectifier. Therefore, RF combining has a higher

RF-to-DC conversion efficiency and output DC power. This observation was made in [27] and is shown here to also hold in the presence of more complex input waveform.

It is worth noting that the proposed algorithms for DC and RF combinings are robust to the imperfect CSI case. To show that, we evaluate the average output DC power for the proposed Algorithms 1, 2, and 3 and the benchmark algorithms with perfect CSI and imperfect CSI. Particularly, the imperfect CSI is modeled as

$$\hat{\mathbf{H}}_n = \sqrt{1 - \tau^2} \mathbf{H}_n + \tau \tilde{\mathbf{H}}_n \quad (75)$$

where \mathbf{H}_n denotes the perfect CSI and $\tilde{\mathbf{H}}_n$ denotes the estimation error with each entry following i.i.d. complex Gaussian distribution with zero mean and unit variance. $\tau \in [0, 1]$ indicates the inaccuracy of the CSI and we set $\tau = 0.1$ in the evaluation. The evaluation results with perfect and imperfect CSI are shown in Fig. 7. We can find that the performance gap between the perfect and imperfect CSI cases are very small for all the proposed algorithms and benchmarks at different numbers of antennas and numbers of frequencies, which shows that the proposed algorithms are robust to the imperfect CSI. Therefore, all the observations and conclusions drawn from the perfect CSI case still hold for the imperfect CSI case.

It is also worthwhile evaluating the received RF power for the different waveform and beamforming designs to understand the crucial role played by the rectenna nonlinearity. Recall again that the linear rectenna model assumes a constant RF-to-DC conversion efficiency, for which maximizing the output DC power is equivalent to maximizing the received RF power. Fig. 8 displays the received RF power averaged over channel realizations versus the number of receive antennas Q for different numbers of transmit antennas M and different numbers of frequencies N . We make the following observations. *First*, the ASS based DC combining has the same received RF power as the ASS based RF combining. This is because they all use the SVD of channel matrix \mathbf{H}_n and choose the strongest channel. This is also consistent with the conclusion in [27] that DC combining has the same performance as RF combining if the linear rectenna model is considered. *Second*, the OPT waveform and beamforming based DC combining (or RF combining) has less received RF power than the ASS based DC combining (or RF combining). This is because OPT waveform and beamforming based DC or RF combining is optimized with the nonlinear rectenna model while the ASS based DC or RF combining is optimal for the linear rectenna model. *Third*, the analog receive beamforming has less received RF power than the general receive beamforming which is because the constraints of analog receive beamforming (45) and (46) is more restrictive.

Based on the above observations from Fig. 6 and Fig. 8, we can find that maximizing the received RF power does not mean maximizing the output DC power due to the rectenna nonlinearity. Therefore, we should consider and leverage the rectenna nonlinearity in WPT to increase the output DC power. This behavior has been extensively emphasized in [6], [41], [29] but finds further consequences in the multi-sine MIMO WPT. To conclude, the rectenna nonlinearity can be leveraged by using multi-sine waveform with DC and RF combinings

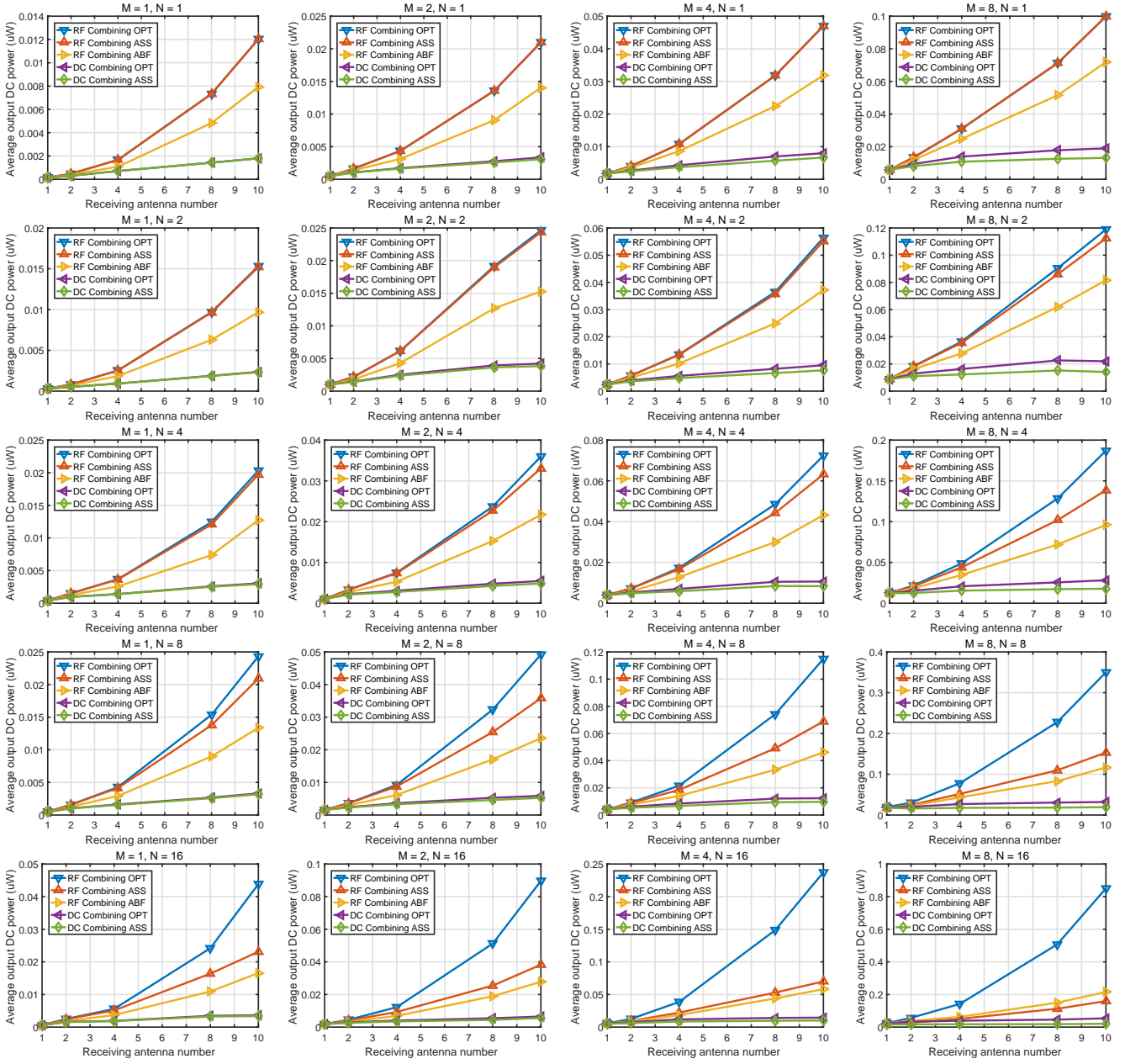


Fig. 6. Average output DC power versus the number of receive antennas Q for different numbers of transmit antennas M and different numbers of frequencies N based on the nonlinear rectenna model.

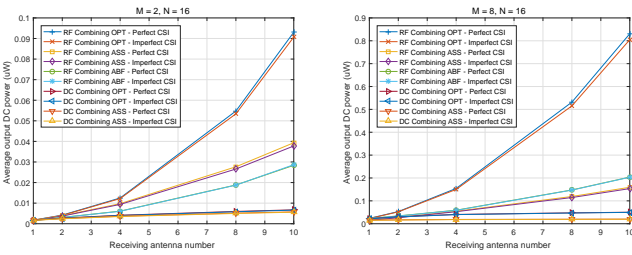


Fig. 7. Average output DC power with perfect CSI and imperfect CSI based on the nonlinear rectenna model.

while RF combining can leverage the rectenna nonlinearity more efficiently.

B. Accurate and Realistic Performance Evaluations

The second type of evaluations uses the circuit simulation solver ADS to accurately model the rectenna so as to validate the joint waveform and beamforming optimization with the DC and RF combinings and the rectenna nonlinearity model.

To that end, in DC combining, for a given channel realization, we first optimize the waveform and beamforming in Matlab so that we can find the RF signal received by each receive antenna. Then, in ADS, we input the RF signal received by each receive antenna to a realistic rectifier as shown in Fig. 9. Hence Q rectifiers as shown in Fig. 9 are used. The output DC power for each rectifier will be solved by ADS so that the total output DC power can be computed. In RF combining, we compute the output DC power in a similar way

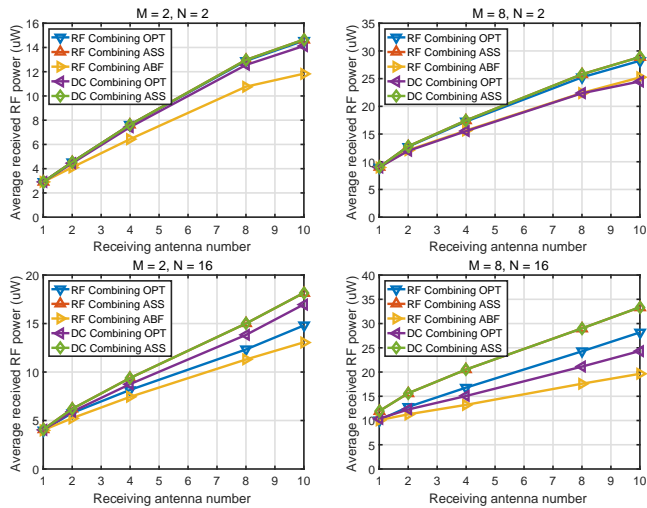


Fig. 8. Average received RF power versus the number of receive antennas Q for different numbers of transmit antennas M and different numbers of frequencies N

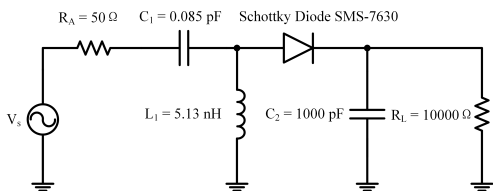


Fig. 9. Rectenna with a single diode and L-matching network used for circuit evaluation in ADS.

but only one rectifier as shown in Fig. 9 is used to rectify the combined RF signal in ADS. The rectenna circuit contains a voltage source, an antenna impedance, an L-matching network, a Schottky diode SMS-7630, a capacitor as low-pass filter, and a load resistor. The L-matching network is used to guarantee a good matching between the rectifier and the antenna and to minimize the impedance mismatch due to variations in frequency and input RF power level. With the SPICE model of SMS-7630, the values of the capacitor C_1 and the inductor L_1 in the matching network are optimized in ADS to achieve a good impedance matching. The output capacitor is chosen as $C_2 = 1000$ pF and the load resistor is chosen as $R_L = 10$ k Ω .

We now evaluate the performance of the multi-sine MIMO WPT system with DC and RF combinings using the accurate rectenna modeling in ADS. Again, we consider two DC combinings (based on OPT and ASS) and three RF combinings (based on OPT, ASS, and ABF). Fig. 10 displays the output DC power averaged over channel realizations versus the number of receive antennas Q for different numbers of transmit antennas M and different numbers of frequencies N based on ADS. We can make the following observations which are similar to the observations in Fig. 6.

First, the output DC power increases with the number of transmit antennas and the number of receive antennas in both DC and RF combinings.

Second, the output DC power increases with the number of frequencies. Compared with the beamforming only design ($N = 1$), the jointly waveform and beamforming design ($N >$

1) is shown to provide a higher output DC power. Specifically, for OPT DC combining, the relative gain of the joint waveform and beamforming design over the beamforming only design can exceed 100% when $N = 16$ and can reach to 180% when $M = 2$, $N = 16$, and $Q = 2$, while for OPT RF combining, the relative gain can exceed 100% when $N \geq 8$ and can reach to 180% when $M = 2$, $N = 16$, and $Q = 2$.

Third, for DC combining, the OPT waveform and beamforming achieves higher output DC power than the ASS based waveform and beamforming. The relative gain of OPT DC combining versus ASS DC combining can be up to 75% when $M = 8$, $N = 16$, and $Q = 10$.

Fourth, for RF combining, the OPT general receive beamforming achieves higher output DC power than the ASS based general receive beamforming. The relative gain of OPT RF combining versus ASS RF combining can be up to 71% when $M = 8$, $N = 8$, and $Q = 10$. In addition, the general receive beamforming outperforms the analog receive beamforming.

Fifth, RF combinings lead to higher output DC power than DC combinings, especially when the number of receive antennas goes large. The relative gain of OPT RF combining versus OPT DC combining increases with N until $N > 8$ due to the breakdown effect of the diode [6] and it can exceed 100% when $Q \geq 4$ and can be up to 550% when $M = 2$, $N = 8$, and $Q = 10$.

The explanations for these observations can be found in the first type of evaluations. It is worth noting that the values of average output DC power shown in Fig. 6 and Fig. 10 are different because the two types of evaluations are calculated by different models. For the first type of evaluations shown in Fig. 6, the average output DC power is calculated by using the nonlinear rectenna model (5). It should be noted that the rectenna model (5) is derived based on some simplifications and assumptions (detailed in [7]) so that it can characterize the rectenna nonlinearity and optimize the waveform and beamforming in a simple and tractable manner. However, this does not mean that the model in (5) is accurate enough to predict the rectifier output DC power using $P_{\text{out}} = v_{\text{out}}^2/R_L$ where R_L refers to the load resistance. Nevertheless, the model and its benefits in optimizing waveform and beamforming have been validated by circuit simulations in [6], [8], [27], [42] and experimentally in [42], [43]. On the other hand, for the second type of evaluations shown in Fig. 10, the average output DC power is calculated by simulating a realistic rectenna in the circuit simulation solver ADS. Using ADS does not provide a simple and tractable manner to optimize the waveform and beamforming but it can accurately simulate the output DC power. Therefore, we use it to verify the waveform and beamforming optimized by using the nonlinear rectenna model (5). The similar observations in Fig. 6 and Fig. 10 confirm the usefulness of the rectenna nonlinearity model and show the benefit of the joint waveform and beamforming design which leverages the beamforming gain, the frequency diversity gain, and the rectenna nonlinearity to increase the output DC power.

VII. CONCLUSION AND FUTURE WORKS

In this paper, we consider the joint design of waveform and beamforming for MIMO WPT systems, accounting for

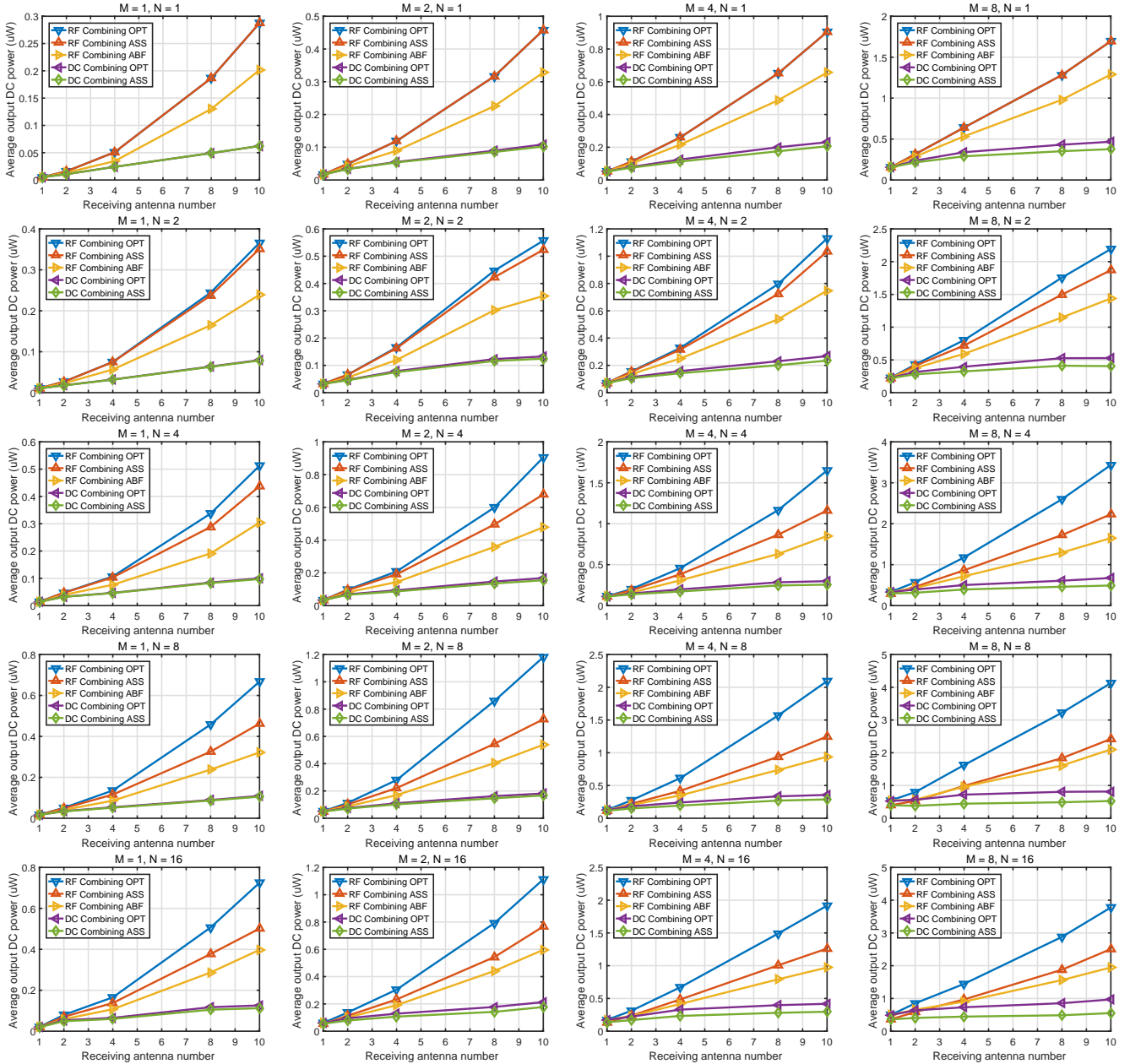


Fig. 10. Average output DC power versus the number of receive antennas Q for different numbers of transmit antennas M and different numbers of frequencies N based on the accurate and realistic circuit simulation.

the rectenna nonlinearity to increase the output DC power. This is the first paper to jointly optimize the waveform and beamforming for MIMO WPT systems. DC combining and RF combining for the multiple rectennas at the receiver are considered.

For DC combining, assuming perfect CSIT and leveraging the nonlinear rectenna model, the waveform and transmit beamforming are jointly optimized with guarantee of converging to a stationary point to maximize the output DC power by using SCA and SDR.

For RF combining, assuming perfect CSIT and CSIR and leveraging the nonlinear rectenna model, the waveform and transmit and receive beamformings are jointly optimized to maximize the output DC power. The optimal transmit and

receive beamforming are provided in closed form and the waveform is optimized with guarantee of converging to a stationary point by using SCA. A practical RF combining circuit consisting of phase shifters and an RF power combiner is also considered. The waveform, transmit beamforming, and analog receive beamforming are jointly optimized with guarantee of converging to a stationary point by using SCA.

We also provide two types of performance evaluations for the joint waveform and beamforming design with DC and RF combinings. The first is based on the nonlinear rectenna model while the second is based on accurate and realistic circuit simulations in ADS. The two evaluations agree well with each other, demonstrating the usefulness of the nonlinear rectenna model, and they show that the output DC power can

be increased by the joint waveform and beamforming design which leverages the beamforming gain, the frequency diversity gain, and the rectenna nonlinearity. It is also shown that the joint waveform and beamforming design provides a higher output DC power than the beamforming only design with a relative gain exceeding 100% when $N = 16$ and reaching to 180% when $M = 2$, $N = 16$, and $Q = 2$. Moreover, RF combining is shown to provide a higher output DC power than DC combining with a relative gain which can be up to 550% when $M = 2$, $N = 8$, and $Q = 10$.

Future research avenues include the following four aspects.

First, designing limited feedback MIMO WPT system. In this paper, we assume the CSI is perfectly known so that the proposed MIMO WPT system architectures with DC and RF combining are simplified and do not contain modules for the CSI acquisition. To acquire the CSI, we need to extra modules in the architectures such as communication module and switch module, and we can use forward-link training or reverse-link training to acquire CSI [1]. To avoid the requirement of CSI, we can consider designing limited feedback MIMO WPT systems in future, as shown in related works on limited feedback MISO WPT systems [11], [44].

Second, unifying the optimizations for DC combining and RF combining. DC combining and RF combining can be unified as a framework named as hybrid combining, where the Q receive antennas are divided into G groups with each group having $Q_G = Q/G$ antennas. In each group, RF combining is used to combine the Q_G receive antennas. Then, DC combining is used to combine the output DC voltage from the G groups. The hybrid combining becomes DC combining when $G = Q$ and becomes RF combining when $G = 1$. Therefore, we can consider developing efficient algorithms for the hybrid combining to unify the optimizations for DC combining and RF combining in future.

Third, considering MIMO WPT systems for a multi-user scenario. In the multi-user scenario, we can optimize the transmit waveform and beamforming and receive beamforming to maximize the weighted sum output DC power of all users. Therefore, we can consider developing efficient algorithms for the multi-user scenario in future.

Fourth, applying MIMO WPT systems in SWIPT [40] and wireless powered communication [45]. Particularly, the proposed algorithms for MIMO WPT systems can be directly applied in SWIPT with time switching scheme [40]. However, with power splitting scheme [40], we need to jointly optimize the waveform, beamforming, and power splitting to maximize the energy and rate, which is more difficult and left as a future work.

REFERENCES

- [1] Y. Zeng, B. Clerckx, and R. Zhang, "Communications and signals design for wireless power transmission," *IEEE Trans. Commun.*, vol. 65, no. 5, pp. 2264–2290, May 2017.
- [2] I. Krikidis, S. Timotheou, S. Nikolaou, G. Zheng, D. W. K. Ng, and R. Schober, "Simultaneous wireless information and power transfer in modern communication systems," *IEEE Communications Magazine*, vol. 52, no. 11, pp. 104–110, 2014.
- [3] W. Lin, R. W. Ziolkowski, and J. Huang, "Electrically small, low-profile, highly efficient, huygens dipole rectennas for wirelessly powering internet-of-things devices," *IEEE Trans. Antennas Propag.*, vol. 67, no. 6, pp. 3670–3679, 2019.
- [4] Y. Hu, S. Sun, H. Xu, and H. Sun, "Grid-array rectenna with wide angle coverage for effectively harvesting RF energy of low power density," *IEEE Trans. Microw. Theory Techn.*, vol. 67, no. 1, pp. 402–413, Jan 2019.
- [5] M. S. Trotter, J. D. Griffin, and G. D. Durgin, "Power-optimized waveforms for improving the range and reliability of RFID systems," in *IEEE Int. Conf. RFID*, April 2009, pp. 80–87.
- [6] B. Clerckx and E. Bayguzina, "Waveform design for wireless power transfer," *IEEE Trans. Signal Process.*, vol. 64, no. 23, pp. 6313–6328, Dec 2016.
- [7] Y. Huang and B. Clerckx, "Large-scale multi-antenna multisine wireless power transfer," *IEEE Trans. Signal Process.*, vol. 65, no. 21, pp. 5812–5827, Nov 2017.
- [8] B. Clerckx and E. Bayguzina, "Low-complexity adaptive multisine waveform design for wireless power transfer," *IEEE Antennas Wireless Propag. Lett.*, vol. 16, pp. 2207–2210, 2017.
- [9] M. R. V. Moghadam, Y. Zeng, and R. Zhang, "Waveform optimization for radio-frequency wireless power transfer," in *IEEE Int. Workshop Signal Process. Adv. Wireless Commun.*, July 2017, pp. 1–6.
- [10] B. A. Mouris, H. Forsell, and R. Thobaben, "A novel low-complexity power-allocation algorithm for multi-tone signals for wireless power transfer," in *2020 IEEE Wireless Communications and Networking Conference (WCNC)*, 2020, pp. 1–6.
- [11] Y. Huang and B. Clerckx, "Waveform design for wireless power transfer with limited feedback," *IEEE Trans. Wireless Commun.*, vol. 17, no. 1, pp. 415–429, Jan 2018.
- [12] K. Kim, H. Lee, and J. Lee, "Waveform design for fair wireless power transfer with multiple energy harvesting devices," *IEEE J. Sel. Areas Commun.*, vol. 37, no. 1, pp. 34–47, Jan 2019.
- [13] B. Clerckx, "Wireless information and power transfer: Nonlinearity, waveform design, and rate-energy tradeoff," *IEEE Trans. Signal Process.*, vol. 66, no. 4, pp. 847–862, Feb 2018.
- [14] M. Varasteh, B. Rassouli, and B. Clerckx, "SWIPT signaling over frequency-selective channels with a nonlinear energy harvester: Non-zero mean and asymmetric inputs," *IEEE Trans. Commun.*, vol. 67, no. 10, pp. 7195–7210, 2019.
- [15] E. Bayguzina and B. Clerckx, "Asymmetric modulation design for wireless information and power transfer with nonlinear energy harvesting," *IEEE Trans. Wireless Commun.*, vol. 18, no. 12, pp. 5529–5541, 2019.
- [16] B. Clerckx, Z. Bayani Zawawi, and K. Huang, "Wirelessly powered backscatter communications: Waveform design and SNR-energy trade-off," *IEEE Communications Letters*, vol. 21, no. 10, pp. 2234–2237, Oct 2017.
- [17] Z. B. Zawawi, Y. Huang, and B. Clerckx, "Multiuser wirelessly powered backscatter communications: Nonlinearity, waveform design, and SINR-energy tradeoff," *IEEE Trans. Wireless Commun.*, vol. 18, no. 1, pp. 241–253, Jan 2019.
- [18] S. Shen and R. D. Murch, "Impedance matching for compact multiple antenna systems in random RF fields," *IEEE Trans. Antennas Propag.*, vol. 64, no. 2, pp. 820–825, Feb. 2016.
- [19] S. Shen, C. Y. Chiu, and R. D. Murch, "A dual-port triple-band L-probe microstrip patch rectenna for ambient RF energy harvesting," *IEEE Antennas Wireless Propag. Lett.*, vol. 16, pp. 3071–3074, 2017.
- [20] S. Shen, Y. Zhang, C.-Y. Chiu, and R. D. Murch, "A compact quad-port dual-polarized dipole rectenna for ambient RF energy harvesting," in *2018 12th European Conference on Antennas and Propagation*, London, United Kingdom, Apr. 2018.
- [21] S. Shen, C. Y. Chiu, and R. D. Murch, "Multiport pixel rectenna for ambient RF energy harvesting," *IEEE Trans. Antennas Propag.*, vol. 66, no. 2, pp. 644–656, Feb. 2018.
- [22] S. Shen, Y. Zhang, C.-Y. Chiu, and R. D. Murch, "An ambient RF energy harvesting system where the number of antenna ports is dependent on frequency," *IEEE Trans. Microw. Theory Techn.*, vol. 67, no. 9, pp. 3821–3832, Sep. 2019.
- [23] S. Shen, Y. Zhang, C. Y. Chiu, and R. Murch, "A triple-band high-gain multibeam ambient RF energy harvesting system utilizing hybrid combining," *IEEE Trans. Ind. Electron.*, vol. 67, no. 11, pp. 9215–9226, 2020.
- [24] U. Olgun, C.-C. Chen, and J. L. Volakis, "Investigation of rectenna array configurations for enhanced RF power harvesting," *IEEE Antennas Wireless Propag. Lett.*, vol. 10, pp. 262–265, 2011.
- [25] J. Xu and R. Zhang, "A general design framework for MIMO wireless energy transfer with limited feedback," *IEEE Trans. Signal Process.*, vol. 64, no. 10, pp. 2475–2488, May 2016.
- [26] G. Ma, J. Xu, Y. Zeng, and M. R. V. Moghadam, "A generic receiver architecture for MIMO wireless power transfer with nonlinear energy

- harvesting," *IEEE Signal Processing Letters*, vol. 26, no. 2, pp. 312–316, Feb 2019.
- [27] S. Shen and B. Clerckx, "Beamforming optimization for MIMO wireless power transfer with nonlinear energy harvesting: RF combining versus DC combining," *IEEE Trans. Wireless Commun.*, vol. 20, no. 1, pp. 199–213, 2021.
- [28] E. Boshkovska, D. W. K. Ng, N. Zlatanov, and R. Schober, "Practical non-linear energy harvesting model and resource allocation for swipt systems," *IEEE Communications Letters*, vol. 19, no. 12, pp. 2082–2085, 2015.
- [29] B. Clerckx, R. Zhang, R. Schober, D. W. K. Ng, D. I. Kim, and H. V. Poor, "Fundamentals of wireless information and power transfer: From RF energy harvester models to signal and system designs," *IEEE J. Sel. Areas Commun.*, vol. 37, no. 1, pp. 4–33, Jan 2019.
- [30] Y. H. Lam, W. H. Ki, and C. Y. Tsui, "Single inductor multiple-input multiple-output switching converter and method of use," Aug. 14 2007, US Patent 7, 256, 568.
- [31] S. Boyd and L. Vandenberghe, *Convex optimization*. Cambridge university press, 2004.
- [32] T. Adali and S. Haykin, *Adaptive signal processing: next generation solutions*. John Wiley & Sons, 2010, vol. 55.
- [33] Y. Huang and D. P. Palomar, "Rank-constrained separable semidefinite programming with applications to optimal beamforming," *IEEE Transactions on Signal Processing*, vol. 58, no. 2, pp. 664–678, 2009.
- [34] B. N. Parlett, "The QR algorithm," *Computing in Science Engineering*, vol. 2, no. 1, pp. 38–42, 2000.
- [35] M. Chiang, C. W. Tan, D. P. Palomar, D. O'neill, and D. Julian, "Power control by geometric programming," *IEEE Trans. Wireless Commun.*, vol. 6, no. 7, pp. 2640–2651, July 2007.
- [36] M. Grant, S. Boyd, and Y. Ye, "CVX: MATLAB software for disciplined convex programming," 2008.
- [37] X. Yu, J. Shen, J. Zhang, and K. B. Letaief, "Alternating minimization algorithms for hybrid precoding in millimeter wave MIMO systems," *IEEE Journal of Selected Topics in Signal Processing*, vol. 10, no. 3, pp. 485–500, 2016.
- [38] F. Sotroghi and W. Yu, "Hybrid analog and digital beamforming for mmwave OFDM large-scale antenna arrays," *IEEE Journal on Selected Areas in Communications*, vol. 35, no. 7, pp. 1432–1443, 2017.
- [39] J. Medbo and P. Schramm, *Channel Models for HIPERLAN/2 in Different Indoor Scenarios*. ETSI EP BRAN 3ERI085B, Mar 1998.
- [40] R. Zhang and C. K. Ho, "MIMO broadcasting for simultaneous wireless information and power transfer," *IEEE Trans. Wireless Commun.*, vol. 12, no. 5, pp. 1989–2001, May 2013.
- [41] B. Clerckx, A. Costanzo, A. Georgiadis, and N. Borges Carvalho, "Toward 1G mobile power networks: RF, signal, and system designs to make smart objects autonomous," *IEEE Microw. Mag.*, vol. 19, no. 6, pp. 69–82, Sep. 2018.
- [42] B. Clerckx and J. Kim, "On the beneficial roles of fading and transmit diversity in wireless power transfer with nonlinear energy harvesting," *IEEE Trans. Wireless Commun.*, vol. 17, no. 11, pp. 7731–7743, Nov 2018.
- [43] J. Kim, B. Clerckx, and P. D. Mitcheson, "Signal and system design for wireless power transfer : Prototype, experiment and validation," *IEEE Trans. Wireless Commun.*, pp. 1–1, 2020.
- [44] S. Shen, J. Kim, C. Song, and B. Clerckx, "Wireless power transfer with distributed antennas: System design, prototype, and experiments," *IEEE Trans. Ind. Electron.*, pp. 1–1, 2020.
- [45] S. Bi, C. K. Ho, and R. Zhang, "Wireless powered communication: opportunities and challenges," *IEEE Communications Magazine*, vol. 53, no. 4, pp. 117–125, April 2015.